

Vitamin A dimers trigger the protracted death of retinal pigment epithelium cells

DM Mihai¹ and I Washington^{*1}

Cellular events responsible for the initiation of major neurodegenerative disorders of the eye leading to blindness, including age-related macular degeneration, Stargardt and Best diseases, are poorly understood. Accumulation of vitamin A dimers, such as *N*-retinylidene-*N*-retinylethanolamine (A2E) in the retinal pigment epithelium (RPE), is one of the earliest measurable events preceding retinal degeneration. However, the extent to which these dimers contribute to tissue degeneration is not clear. To determine if A2E could trigger morphological changes associated with the degenerating RPE and subsequent cell death, we evaluated its toxicity to cultured human RPE cells (ARPE-19). We show that A2E triggered the accumulation of debris followed by a protracted death. A2E was up to ≈ 14 -fold more toxic than its precursor, retinaldehyde. Measurements reveal that the concentration of A2E in the aged human eye could exceed the concentration of all other retinoids, opening the possibility of A2E-triggered cell death by several reported mechanisms. Findings suggest that accumulation of vitamin A dimers such as A2E in the human eye might be responsible for the formation of ubiquitous RPE debris, an early indication of retinal degeneration, and that preventing or reducing the accumulation of vitamin A dimers is a prudent strategy to prevent blindness. *Cell Death and Disease* (2014) 5, e1348; doi:10.1038/cddis.2014.314; published online 24 July 2014

The elucidation of environmental and genetic drivers of RPE senescence has been a persistent goal toward understanding and preventing degenerative disease of the retina. Since their structural elucidation in the 1990s, dimers of dietary vitamin A, in particular *N*-retinylidene-*N*-retinylethanolamine (A2E), have been postulated as chemical triggers, driving retinal senescence and associated degeneration. The eye uses vitamin A as a cofactor to sense light. A striking chemical signature of the aging and degenerating retina is the accumulation of vitamin A dimers in the retinal pigment epithelium (RPE)^{1,2} and underlying Bruch's membrane.³ In rodent models of macular degeneration,^{4–8} high levels of vitamin A dimers correlate with poor retinal health and a variety of mechanisms have been proposed by which dimers of vitamin A may induce retinal toxicity ranging from non specific to direct antagonistic/protagonistic mechanisms.^{9–16} As a cationic amphiphilic pyridinium, A2E has been shown to solubilize lipid membranes, inactivate lysosomes by increasing lysosomal pH, and accumulates in the negatively charged mitochondrial compartment. Once dimerized, the special orientation of the polyene chains make them especially susceptible to oxidative degradation¹⁶ leading to secondary reactive aldehyde and epoxide toxicants.¹⁷ Direct reported mechanisms of A2E toxicity include, acting as an agonist for retinal pigment epithelium-specific 65-kDa protein,¹⁸ retinoic acid receptors,¹⁰ cyclooxygenase-2,¹⁹ and covalent modification of biomolecules,^{20,21} among others.

Despite data demonstrating that dimers of vitamin A can disrupt cellular homeostasis, there is less direct evidence supporting their role as primary drivers of retinal senescence. More recently, based on studies in ARPE-19 cells, it has been

proposed that A2E's chemical precursor, vitamin A aldehyde (retinaldehyde), might play a role in the degenerative process and that A2E might be a benign biomarker of increased levels of retinaldehyde.^{16–18} To determine if A2E could chemically trigger the degenerative process in the retina, we explored the acute and long-term toxicity of A2E to human retinal pigment epithelium (RPE) cells *in vitro*. ARPE-19 cells treated with A2E showed degraded mitochondria, accumulated glycogen and lipofuscin debris, and underwent a protracted, dose-dependent death over several days to months. These data suggest that A2E can trigger the accumulation of lipofuscin-like debris in the *in vivo* RPE and can be detrimental to the retina's health. Data further reveal that increasing concentrations of A2E in the RPE potentially plays a larger role in retinal senescence than previously thought.

Results

A2E in the aged human eye. To determine the approximate amount of A2E in the aged human eye, we quantified A2E from seven eyes of donors between 67 and 87 years of age. Figure 1a shows representative chromatograms of a solution of synthetic A2E and of an organic extract from a human eye. All peaks from the eye extract displayed double-arm absorption spectra characteristic of dimerized vitamin A. We found the human eyes to contain 54 ± 16 nmoles of A2E per eye. Over 95% of A2E was recovered from the eyes as additional extractions recovered less than 0.02 nmoles of A2E per eye. The limit of detection for A2E was 3 pmoles of A2E on column. The same eyes contained an average of

¹Department of Ophthalmology, Columbia University Medical Center, New York, NY 10032, USA

*Corresponding author: I Washington, Department of Ophthalmology, Columbia University Medical Center, 160 Fort Washington Avenue, New York, NY 10032, USA. Tel: +1 212 342 9060; Fax: +1 212 342 9060; E-mail: iw2101@columbia.edu

Abbreviations: RPE, retinal pigment epithelium; A2E, A vitamin A dimer
Received 10.2.14; revised 24.5.14; accepted 29.5.14; Edited by A Verkhatsky

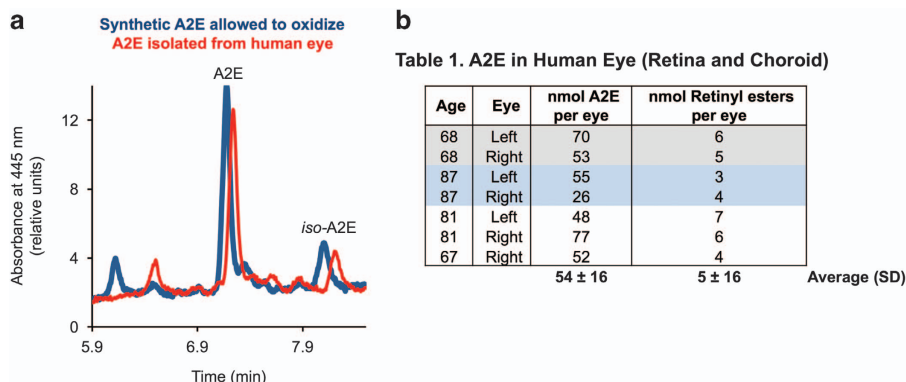


Figure 1 Concentrations of A2E can exceed vitamin A esters in the aged human eye. (a) Representative LC trace of A2E and an extract from an 87-year-old eye. A2E and oxidized A2E were defined as all peaks shown in the chromatogram. Peaks from A2E isomers and their oxidation products (blue line) overlapped with peaks from extracts from human eyes (red line), with the exception of the first peak. The first eluting peak, seen in the oxidized A2E sample, was absent in the human-derived extract. (b) Total amount of A2E and oxidized A2E measured in the human eyes

5 ± 1 nmoles of retinyl esters per eye, within the range of the amount of retinyl esters reported from human eyes (9 ± 4 pmoles per eye).²² We found significantly less A2E in the 3–5-year-old bovine eye (10 ± 1 pmoles per eye; $n=3$) and in the 6-month-old swine eye (2.4 ± 0.4 pmoles per eye; $n=4$). However, the amounts of vitamin A esters were of the same order of magnitude of that found in the human eye (12 ± 0.4 for bovine and 9 ± 3 for swine).

Uptake and metabolism of retinaldehyde and A2E. As a model of the RPE, we used a commercial human RPE cell line, ARPE-19, which we cultured under three conditions: non-confluent (80% confluent), 2 week post confluence and 8 week post confluence (Supplementary Figure S1). As retinaldehyde and A2E are not readily water soluble, we incorporated them into liposomes²³ and determined their bioavailability when added to the culture medium.

The major retinoids detected 15 h after incubating 8-week confluent RPE cells with retinaldehyde were retinoic acid, all-*trans*-retinol, 11-*cis*-retinol and retinol esters (Figure 2a). Negligible amounts of retinaldehyde were found, suggesting retinaldehyde had been either reduced or oxidized. The ratios of retinol, retinoic acid, and retinyl ester changed with time and were dependent on culturing conditions (Supplementary Figure S2). In general, longer incubation times resulted in more retinol and retinoic acid. We were not able to detect any retinoids in control cultures in which retinaldehyde was not added to the medium.

Conversely, cells incubated with A2E incorporated A2E over several days (Figures 2b and c). During 14 days of incubation, 30% (4.5 pmoles/ mm^2) of A2E in the media had been incorporated into cells (Figure 2c). Oxidized A2E was also detected in the cells (Figure 2b). The incorporated A2E remained stable. For example, after incubating cells with 16 pmoles/ mm^2 of A2E for 2 days and then washing the cells, 1.2 pmoles/ mm^2 of A2E had been incorporated. After an additional 14 days, we measured the same amount of cellular A2E (A2E day 14: 1.2 ± 0.2 pmoles; $P > 0.5$). However, when A2E was incubated in media alone for 14 days, 16% of A2E had degraded.

Acute toxicity of A2E and retinaldehyde. Figures 3a and b show representative light microscopy images of cells scored as alive (a) or dead (b) after their incubation with A2E. Figure 3c plots the number of days required to reach cell death for cells cultured for up to 3 weeks post exposure to A2E at various concentrations (horizontal axis). High concentrations of A2E (200 – 600 pmoles/ mm^2) induced cell death within days, whereas cell death occurred after 3 weeks with lower concentrations (88 – 176 pmoles/ mm^2). For the lowest tested concentrations (29 – 59 pmoles/ mm^2), no toxicity was observed during the 3-week test period. After visual inspection, we confirmed cell viability through the resazurin assay (Supplementary Figure S3). The dose of A2E at which the rate of resazurin reduction was halved (EC_{50}) was 57 – 66 pmoles/ mm^2 for cells cultured under all three culturing conditions (Figures 3e–g).

Similarly, we treated cells with liposomal retinaldehyde. Contrary to A2E, toxic levels of retinaldehyde induced cell death within 2 days as measured by visual inspection and resazurin assay (Figure 3d). Longer incubation times did not affect the EC_{50} . The EC_{50} varied with the maturity of the cell culture. For non-confluent cells, the EC_{50} was 46 pmoles/ mm^2 (Figure 3h). For 2-week confluent cells, the EC_{50} increased to 114 pmoles/ mm^2 (Figure 3i), while for 8-week confluent cells, EC_{50} reached 310 pmoles/ mm^2 , nearly sixfold the EC_{50} of non-confluent cells (Figure 3j). When the 8-week confluent cells were treated with the lower concentrations of retinaldehyde (88 – 176 pmoles/ mm^2), resazurin reduction rates were significantly faster than control cells not treated with retinaldehyde (Figure 3j).

Morphological changes in cultured RPE cells in response to chronic repeat A2E exposure. To determine if A2E could induce morphological changes *in vitro* commonly associated with the degenerating *in vivo* RPE, we investigated changes in RPE morphology in response to sub-toxic treatment with A2E. Retinal hyperautofluorescence is considered an early indicator of pathology. Cells incubated with A2E for 24 h exhibited localized and spherical autofluorescence (Figure 4a), while fluorescence was absent in cells cultured without A2E. Cells treated repeatedly with A2E

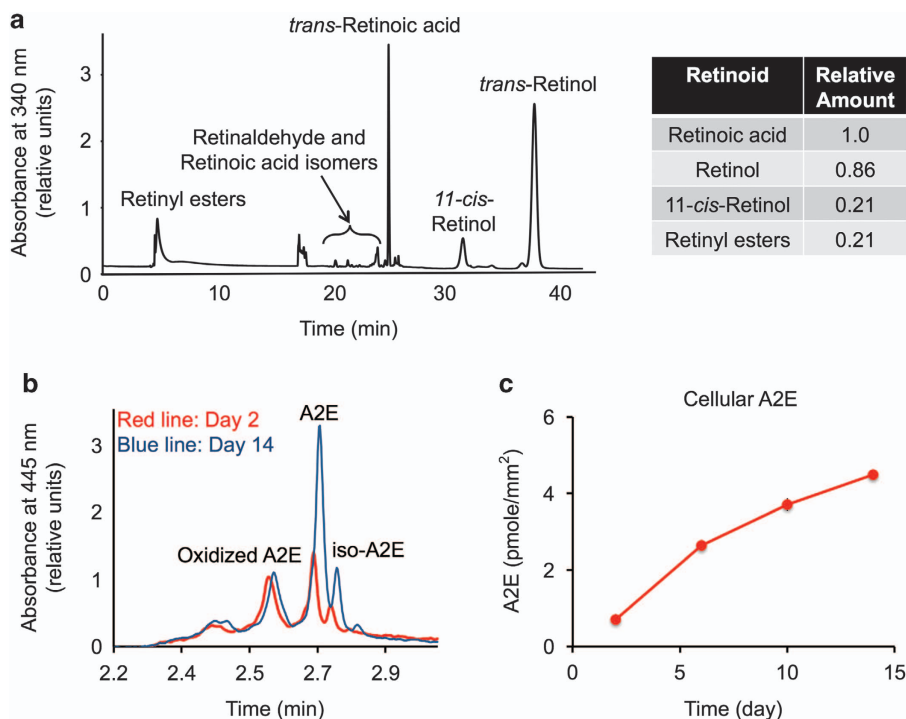


Figure 2 Retinaldehyde is metabolized, A2E accumulates. **(a)** Representative HPLC chromatogram of retinoids in the combined cell culture medium and cells 16 h after incubation with 64 pmoles of retinaldehyde/mm² of culture plate. Relative amounts of synthesized retinoids are shown. Under the HPLC conditions employed, retinaldehyde isomers overlapped with the *cis*-, *trans*-isomers of retinoic acid. Cells were cultured for 8 weeks on polystyrene. **(b)** Representative HPLC chromatograms of A2E extracted from cultured ARPE-19 cells. We incubated 2-week confluent cultures with 16 pmoles/mm² A2E. At 2 and 14 days, we removed the media and we quantified cellular A2E by HPLC. Peaks representing A2E and oxidized A2E are labeled. **(c)** Plot showing A2E accumulation with time. We incubated 2-week confluent cultures with 16 pmoles A2E/mm² surface area. At the times shown, we washed the cells and quantified cellular A2E by HPLC

for longer periods (3.5 months) showed diffuse, particulate, and demarcated areas of autofluorescence (Figure 4b), while age-matched control cells not treated with A2E showed no autofluorescence (Supplementary Figure S4). The above data are consistent with the notion that vitamin A dimers such as A2E are potentially major contributors to retinal hyperautofluorescence in humans.

Figures 5 and 6 show the ultrastructure of cells at 1 and 4 months of age when not treated (controls) or treated with A2E, respectively. At 1 month (Figures 5a–d), the control cells appeared flat, in a monolayer with thin apical and basement processes and with microvilli or finger-like projections on the apical and basal surfaces. Primary lysosomes, mitochondria, rough and smooth endoplasmic reticula, and lipid bodies were distributed throughout the cytoplasm. The cells were without melanin or tight junctions. At 4 months (Figures 5e–h), Golgi apparatus, mitochondria, and rough and smooth endoplasmic reticula were more developed and prominent. Pinocytotic vesicles and multivesicular inclusions were also observed in the cytoplasm at this stage. Glycogen was more prominent and distributed randomly throughout the cytoplasm. Areas of cell multilayering, up to three cell layers thick, could also be seen. Tight junctions began to form at cells joined at the apex and laterally.

Conversely, at 1 month (Figures 6a–f), A2E-treated cells contained abundant, randomly arranged glycogen deposits, and large glycogen pools up to 1 μ m in diameter. Vacuoles were apparent around the glycogen deposits. Cell multilayering was observed, contrary to what was seen in

age-matched controls. Cell shape was more irregular and the apical and basement processes were longer and more numerous than in control cells. More lipid droplets and lysosomes were found compared with control cells. The lysosomes in the A2E-treated cells were more heterogeneous with varying electron densities. In the 4-month group (Figure 6g), degenerated dead cells were apparent, although absent in age-matched controls. Cells grew in multilayers, up to five layers in some cases. Glycogen and associated vacuoles were more apparent, with vacuoles increasing in size. There was a dramatic increase in heterogeneous lysosomal bodies. However, lipid droplets decreased compared with A2E-treated cells at 1 month. Atrophic mitochondria presented as multilayered or laminated bodies (Figures 6h–k). Some of these laminated bodies contained paracrystalline inclusions (Figure 6i).

A2E-treated cells showed 110% greater area of Schiff base staining compared with control cells, confirming an increase in glycogen (Figure 7). No fluorescence was observed when we reacted A2E-treated cells with the Schiff reagent in the absence of periodic acid oxidation (Supplementary Figure S5), ruling out potential contribution of native aldehydes to the pararosaniline-Schiff fluorescence.

Discussion

We found that the amount of A2E in the 70–87-year-old eye (54 ± 16 nmoles per eye) can exceed that of vitamin A. This amount of A2E was similar, on a per retinal surface area basis,

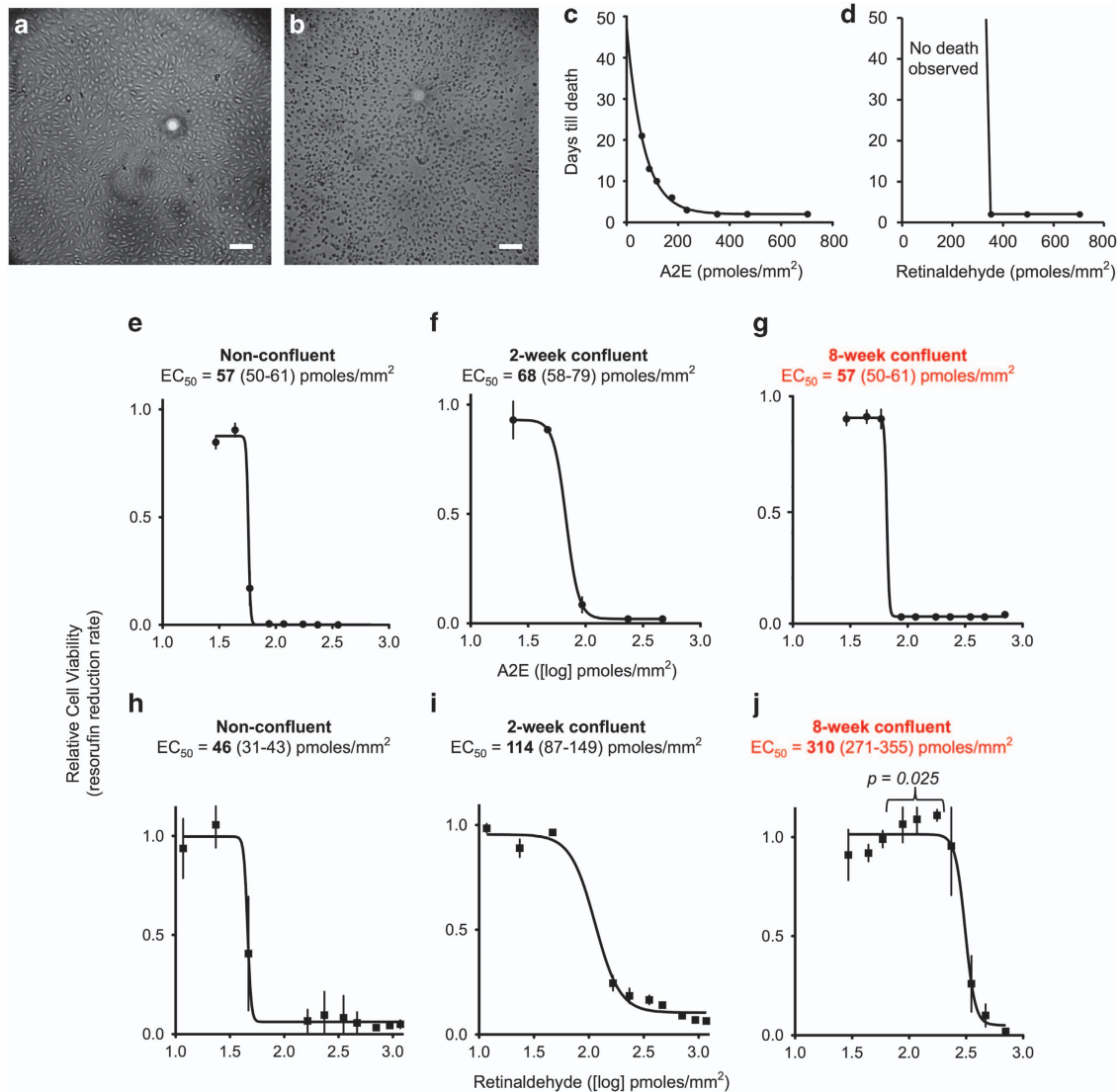


Figure 3 Relative acute toxicities of A2E and retinaldehyde. Representative light micrographs of cells scored as alive (a) and dead (b). Scale bar, 100 μm. (c and d) Plots showing time to death for 8-week confluent ARPE-19 cells treated with varying concentrations of A2E or retinaldehyde as evaluated by visual inspection according to panels a and b. We grew cells in gelatin-coated 96-well plates for 8 weeks, then treated them with a single dose of the shown amounts of A2E or retinaldehyde, added to the cell culture media. Over the next 21 days, we visualized the cells every 2–3 days for viability. Media were not changed throughout the experiment. (e–g) Dose-response curves for 8-week confluent ARPE-19 cells treated with A2E for 21 days. We plotted the resazurin reduction rates of A2E-treated cells relative to those for control cells not given A2E, against the respective A2E dose. Mean and standard errors are shown. EC₅₀: concentration at which the resazurin reduction rate dropped by 50%. (h–j) Dose-response curves for three groups of ARPE-19 cells treated with retinaldehyde. Cells were grown to the desired stage in 96-well plates and then treated with a single dose of retinaldehyde. After 7–21 days, resazurin reduction rates were measured and the rates were used to generate dose-response curves, as described for A2E in d. Retinaldehyde killed cells within 2 days. Unlike for A2E, incubation for 21 days did not lower or otherwise change the EC₅₀. In j, *P*-values compare points highlighted to the lowest dose of retinaldehyde used

as the amount of A2E reported in the mouse model of Stargardt disease,²⁴ but exceeded estimates from previous reports in humans. In pooled isolated RPE/choroids from donors above 40 years of age, an average 0.7–1.13 nmoles of A2E per eye was estimated.^{2,25} In donors with Best vitelliform macular dystrophy, the concentration of A2E was estimated to be approximately 4.5 nmoles per eye.²⁶ We calculated an extinction coefficient at 435 nm of 15,146 M⁻¹/cm¹ measured in ethanol. This value is approximately half of what was previously reported.²⁵ However, halving extinction coefficient would only halve our calculated amount of A2E. The propensity of A2E to exercise its full toxicity spectrum is presumably dictated by its concentration. As such, the

relatively large amounts of A2E found in the eye opens the possibility of A2E triggering retinal death by a variety of proposed mechanisms.

Suggestions that vitamin A, as retinaldehyde, rather than its dimers might be a primary driver of retinal degeneration, resulted from studies comparing toxicities of retinaldehyde and A2E in cultured ARPE-19 cells. Maeda *et al.*²⁷ and Wielgus *et al.*²⁸ observed that retinaldehyde added to the cell culture media killed RPE cells but that A2E at the same concentrations did not appear toxic. This finding was partially corroborated by Suter *et al.*²⁹ and Sparrow *et al.*³⁰ who reported that A2E-induced cell death occurred at higher concentrations in the cell culture medium than reported by

others for retinaldehyde. Conversely, Doyle *et al.*³¹ and Ablonczy *et al.*³² reported no toxicity from retinaldehyde at concentrations reported toxic by Maeda *et al.*²⁷ and Wielgus *et al.*^{27,28}

Here, similarly, we compared the effects of a single dose of A2E or retinaldehyde to RPE viability in culture.

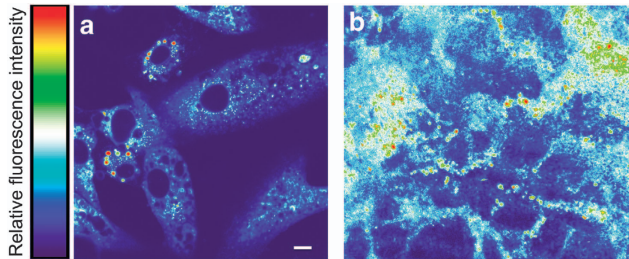


Figure 4 A2E treatment induces autofluorescence. Excitation = 488 nm; emission = 511–742 nm. Scale bar, 10 μm . The colored bar represents relative fluorescence intensity, red being the highest and purple being non-fluorescent. (a) Light micrograph of 50% confluent ARPE-19 cells grown on a collagen-coated glass, treated with A2E, and visualized 24 h later. No autofluorescence was observed in cells not incubated with A2E and imaged under identical conditions (i.e., the entire image was purple). (b) ARPE-19 cells aged for 4 months on polycarbonate mesh, treated weekly with A2E for up to 4 months, fixed with methanol, and imaged via confocal fluorescence microscopy as in a. Diffuse, particulate, and demarcated areas of autofluorescence and an overall increase in autofluorescence were observed. No autofluorescence was observed in control cells not incubated with A2E but otherwise treated and imaged identically (Supplementary Figure S4)

Cells incorporated and stored A2E and did not appear to metabolize it. Relatively minute concentrations of A2E depressed cellular energetics and resulted in a protracted cell death, occurring up to 3 weeks after initial exposure to A2E. Previous toxicity studies evaluated shorter times post exposure (2 days), thus seemingly underestimating the toxicity of A2E toward the RPE. The observed protracted A2E-induced cell death is perhaps consistent with the protracted degeneration occurring in diseases such as age-related macular degeneration, where A2E and similar dimers of vitamin A are known to accumulate over a lifetime.

A2E toxicity was independent of cell maturity or culturing conditions. Using RPE cells cultured past confluence, we found A2E to be up to sixfold more toxic than retinaldehyde. Because we did not correct for the actual uptake of A2E into the cells, we perhaps underestimated its relative toxicity. For example, after 14 days of a single-dose administration, a fraction ($\approx 30\%$) of A2E was incorporated into the cells, so that the reported EC_{50} of 66 pmoles/ mm^2 could be reduced to about 22 pmoles/ mm^2 when corrected for A2E uptake. This concentration is about 14 times lower than what was required for retinaldehyde-induced cell death. The amount of A2E found in the eyes of older individuals was around the same order of magnitude to that needed to induce a protracted cell death *in vitro*.

In contrast, retinaldehyde-induced toxicity, if any, occurred relatively instantly, happening within 2 days,

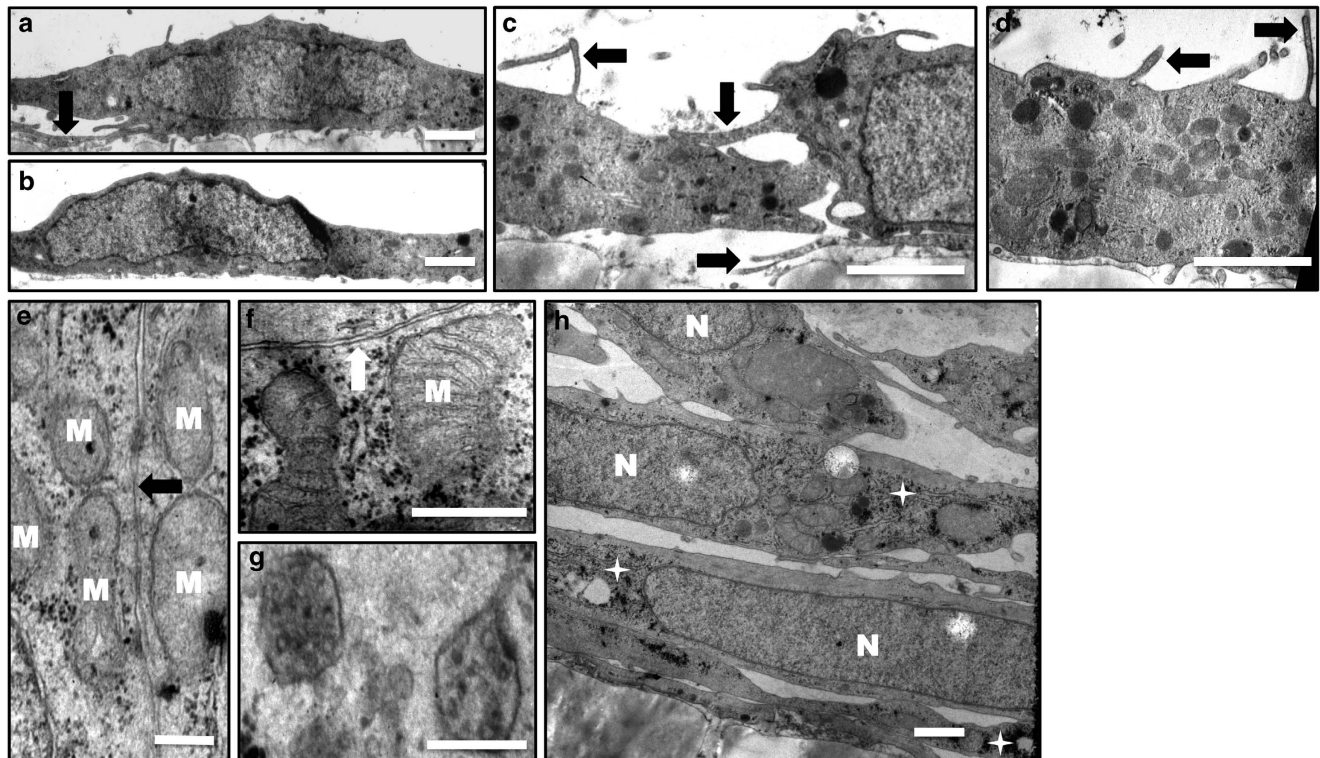


Figure 5 Control RPE cells. Representative electron micrographs of ARPE-19 cells cultured for 1 month (a–d) and 4 months (e–h). (a and b) At 1 month, cells were monolayer, scale bar, 1.0 μm . (a, c and d) Apical and basement processes could be seen (arrows). (c and d) Sporadic electron-dense inclusions were present. Scale bar, 1.0 μm . (e and f) At 4 months, tight junctions began to form (arrows), mitochondria became more defined (e) M: mitochondria; scale bar, 0.25 μm , (f) scale bar, 0.3 μm . (g) Multivesicular inclusions were seen. Scale bar, 0.175 μm . (h) Cell multilayering and randomly distributed glycogen (stars) are shown. N: nucleus, scale bar, 1 μm

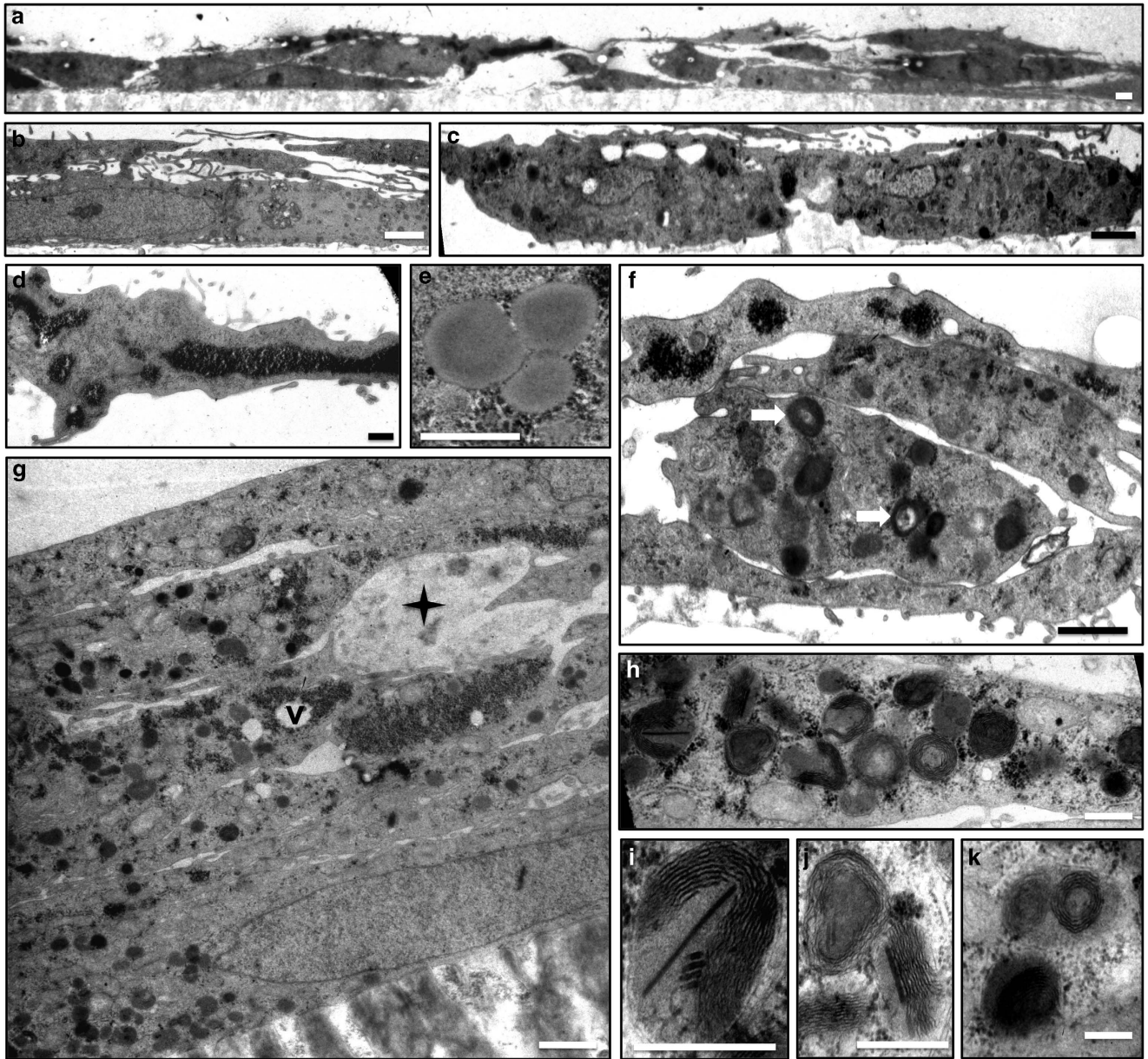


Figure 6 A2E induces morphological changes associated with retinal degeneration. Representative electron micrographs of ARPE-19 cells treated weekly with A2E for 1 month (a–f) and 4 months (g–k). Cells treated with A2E displayed morphological changes associated with the retinal degeneration. (a) Cell multilayering, up to three layers. Scale bar, 1.0 μm . (b) Long apical and basement processes. Scale bar, 1.0 μm . (c) Irregularly shaped cells. Scale bar, 1.0 μm . (d) Large, electron-dense, granular glycogen pools were seen. In addition, glycogen was observed in discrete alpha patterns and randomly distributed throughout the cytoplasm. Scale bar, 1.0 μm . (e) Three lipoidal inclusion bodies along with 25–35 nm electron-dense glycogen particles are shown. Scale bar, 0.5 μm . (f) Cell multilayering, glycogen bodies, electron-dense inclusion bodies with electron opaque cores (arrows). (g) Cell multilayering (five layers are shown.): atrophic cells (star), glycogen bodies and varying size, vacuole formation (v) around glycogen bodies and many lysosomes of varying electron densities are shown. (h–k) Laminated bodies. Scale bar, 0.6 μm . (i) A laminated body with paracrystalline inclusions. Scale bar, 0.4 μm . (j) A close-up of laminated inclusions shown in k. Scale bar, 0.6 μm

at high doses. But at sub-toxic doses, retinaldehyde actually increased cellular energetics. For these sub-toxic doses, retinaldehyde was found to be metabolized within hours, consistent with retinaldehyde being a chemical symbiont of the retina, required for proper homeostasis, its absence or partial depletion resulting in retinal degenerations and blindness. Retinaldehyde toxicity was depended on culturing conditions and was relatively toxic only to non-confluent cells. However, when cells were cultured differently (matured past

confluence), retinaldehyde toxicity decreased by nearly sixfold.

In vivo, very little ‘free’ retinaldehyde exists.³³ In the eye, retinaldehyde is found almost entirely bound to phosphatidylethanolamine or to one of several proteins found inside, outside, and on the surface of the RPE. Such proteins include opsin, cellular retinaldehyde-binding protein 1, the retinal G protein-coupled receptor (RGR),³⁴ cellular retinol-binding protein type I (CRBP-I), and serum retinol-binding protein

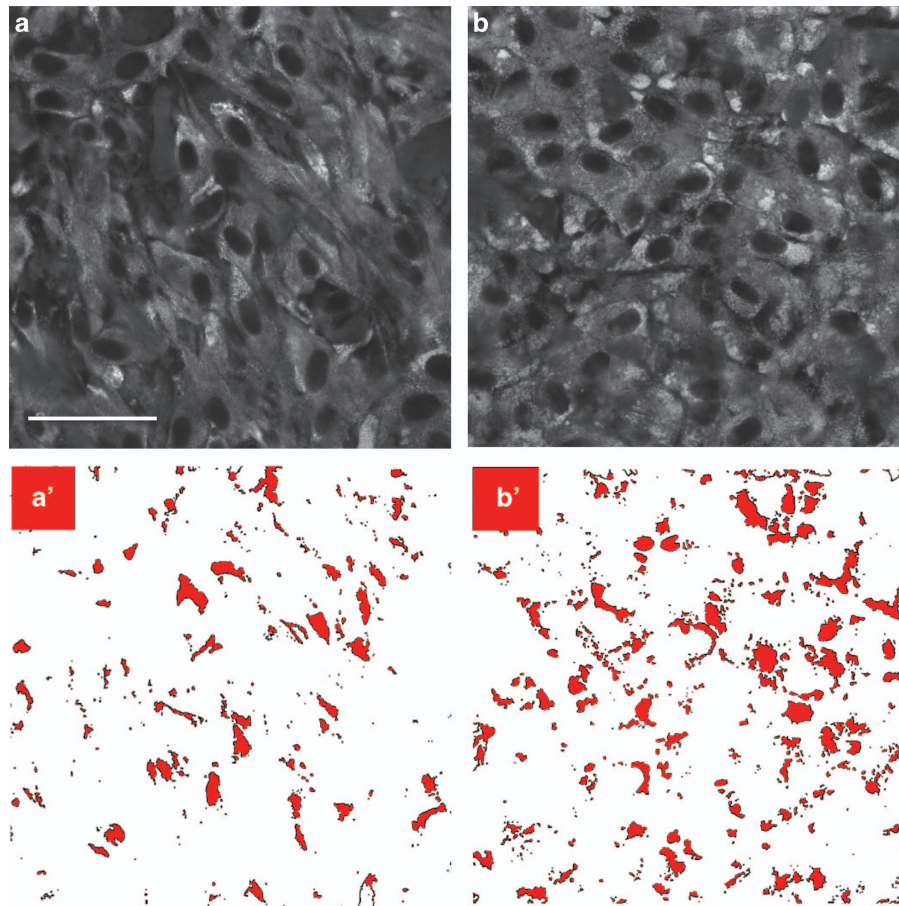


Figure 7 A2E increases glycogen stores. Fluorescence microscopy images of (a) control and (b) A2E-treated ARPE-19 cells fixed in methanol, oxidized with periodic acid, reacted with pararosaniline, and visualized via confocal fluorescence microscopy under identical acquisition conditions. Scale bar, 35 μm . Cells were cultured for 4 months on polycarbonate mesh and either treated weekly with liposomal A2E or liposomes alone (control). Glycogen is seen as areas of increased fluorescence intensity (lighter areas). Excitation = 638 nm, emission = 660–737 nm. Control and A2E-treated cells fixed in methanol alone, or reacted with pararosaniline, but not oxidized with periodic acid, were not fluorescent at these wavelengths Supplementary Figure S5. To quantify glycogen in panels a and b, the images were converted into binary images a' and b', respectively, where black represents fluorescence intensity or glycogen deposits above a defined threshold. Treated cells had a 110% increase in total area of fluorescence (64 358 control versus 133 219 treated) as well as 110% increase in fluorescence area fraction (6 versus 13)

(RBP). For example, the concentrations of proteins available to bind to retinaldehyde in the interphotoreceptor matrix (interphotoreceptor retinoid-binding protein (IRBP), serum albumin, and RBP) exceed that of retinaldehyde.³⁵ The sequestration of retinaldehyde by its binding proteins would, presumably, limit any potential toxicity. Furthermore, *in vivo*, retinaldehyde is actively transported out of the RPE mediated by IRBP and RBP.³⁶ Such transport, would also presumably limit toxicity. Furthermore, retinaldehyde can be reduced or oxidized by one of several retinaldehyde dehydrogenases (RDHs), which reside inside the RPE or in the neighboring photoreceptors. Retinaldehyde sequestration, transport, and/or its oxidation or reduction all limit the exposure of the RPE to 'free' retinaldehyde, thus limiting its toxicity in the eye.

Many of the above-listed retinaldehyde/retinoid binding and visual cycle-processing proteins only begin to be synthesized in cultures confluent for several months.^{37–39} RPE cultures can vary in their rates of biotransformation, distribution, and excretion of retinaldehyde, potentially explaining the variability in retinaldehyde toxicity to differentially cultured RPE

cells. Toxicity studies in models lacking the above proteins would overestimate retinaldehyde toxicity. For example, retinaldehyde-induced toxicity diminishes in kidney (HEK293) cells when the cells express retinol dehydrogenase 12,⁴⁰ an enzyme able to convert retinaldehyde into retinol. Even freshly isolated RPE cells can lose their ability to synthesize 11-*cis*-retinoids depending on culture conditions.⁴¹ Conflicting results of retinaldehyde toxicity is presumably a result of differences in retinaldehyde metabolism due to culture maturity or culturing conditions similar to as observed here. At homeostasis, the RPE is estimated to contain 3.3 μM of retinaldehyde.⁴² Given the above-listed redundant mechanisms of retinaldehyde use, the *in vivo* eye can potentially process large fluxes of retinaldehyde. For example, in eye disorders such as Oguchi disease, retinaldehyde fluxes are thought to be high enough to turn the retina yellow,⁴³ although retinal degeneration does not occur.

This work demonstrates that A2E can induce cell death at relatively low concentrations without light exposure. Retinaldehyde⁴⁴ and A2E⁴⁵ have been shown, in culture, to induce greater cell death upon light exposure. We did not investigate

the contribution of light. When comparing light-induced toxicity, in several reports, cells are incubated with retinaldehyde for up to several hours²⁸ to days²⁷ before light exposure. However, in our cell model, RPE cells metabolized retinaldehyde within hours, complicating the interpretation of reports that have used such models to implicate retinaldehyde in light-induced toxicity.

A2E triggers debris. To elucidate the long-term stresses responsible for retinal degeneration, several studies have assessed morphological changes in RPE cells induced by long-term cellular stress. In particular, it has been reported that feeding outer segments to RPE cells leads to an increase in lipofuscin-like bodies.^{46–48} These observations support the hypothesis that lipofuscin accumulates as a result of outer segment phagocytosis. Outer segments, however, comprise a complex biological mixture, including A2E.⁴⁹ Our results demonstrate that A2E itself can be responsible for RPE debris found in the human eye. In this work, the term debris encompasses lipofuscin-like bodies, late-stage lysosomes, abnormal glycogen and lipid deposits, and inclusions that show heterogeneous electron density. As all the above electro-heterogeneous inclusions are seen, to a much lesser extent, in control cells, we here term them collectively 'debris'.

In general, lipofuscin granules are thought to be terminal stages of lysosomal autophagocytosis of mitochondria, glycogen, and lipid droplets.⁵⁰ Thus, the observations that A2E results in the appearance of abnormal mitochondria, glycogen deposits, and lipid droplets is of particular interest. The accumulation of the above debris in A2E-treated cells can be a result of either: (1) dysregulated lysosomal clearance or (2) specific interference with biological pathways responsible for glycogen, lipid, and/or mitochondrial homeostasis. The notion that A2E inhibits lysosomal clearance is consistent with reported biochemical data evaluating lysosomal function in the presence and absence of A2E.^{12,51} However, A2E has also been suggested to directly decrease mitochondrial function^{29,51} and disrupt cellular homeostasis by several mechanisms. The debris may also reflect hindered clearance of the delivered liposomes or may be storage compartments for A2E. A2E, being composed of conjugated double bonds, would be expected to be stained by osmium tetroxide and appear electron dense. At present, we cannot conclude whether debris accumulates because of hindered lysosomal clearance or by direct antagonistic mechanisms. Morphologically, A2E administration leads to similar pathology to that of other cationic amphiphilic drugs, which have been shown to induce the formation of cytoplasmic inclusion bodies in the rat RPE.⁵² Indeed, the high concentrations of A2E compared with vitamin A, found here, in the aging human eye suggest that many of the reported mechanisms of A2E-induced toxicity could be in play.^{9–16}

A2E-induced laminated bodies. The laminated bodies we observe *in vitro* have been noted in the degenerating RPE.^{37,53–55} Such bodies are observed in mitochondria-related maculopathies and are said to be mitochondria at varying stages of atrophy. The lamination representing aberrant mitochondrial cristae derived from the infolded inner

membrane in which protein complexes of oxidative phosphorylation and intermediate metabolism are embedded. Laminated mitochondrial inner membranes have been shown to correlate with increased reactive oxygen species production, changes in membrane potential, and apoptosis.⁵⁶ A2E, a positively charged molecule, can be expected to be attracted to the mitochondria's large negative potential.²⁹ It could be that A2E disrupts mitochondrial architecture, which leads to biochemical defects and mitochondrial atrophy seen in the aging RPE.⁵⁷ Alternatively, such bodies might accumulate due to dysregulated lysosomal clearance.

A2E-induced glycogenesis. In cells treated with A2E, there was an increase in glycogen bodies, as observed structurally and quantified via Schiff base staining. RPE sections from AMD eyes also stain strongly for glycogen.^{58,59} Accumulation of glycogen reflects lower glucose utilization and diminished glycolysis. Glucose is a major energy source for retinal metabolism.⁶⁰ The RPE forms a barrier preventing passive diffusion of glucose from the choroid to the photoreceptors and stores glucose as glycogen.⁶¹ Altered glucose metabolism in the RPE would affect glucose utilization in the neural retina.

Conclusion

The gradual failure of the retinal pigment epithelium and Bruch's membrane has long been suspected to be the primary event leading to retinal degeneration in major age-related and inherited neurodegenerative eye disorders. A common chemical event that occurs at the earliest stage of several neurodegenerative retinal disorders is the dimerization of vitamin A and its accumulation in the RPE and Bruch's membrane. The presented data reveal that dimerized vitamin A, A2E, can induce protracted RPE cell death and can be directly responsible for the genesis of RPE inclusion bodies similar to those observed *in vivo* in the RPE cells of the degenerating retina. Our data show that A2E can induce large-scale cytoplasmic remodeling consistent with previously reported biochemical modes of A2E-induced toxicity. Data suggest that A2E accumulation in the RPE can be an early and primary driver of several forms of macular degeneration, and that targeting A2E and other vitamin A dimers for their reduction is a prudent therapeutic strategy.

Materials and Methods

A2E in the aged human eye. All procedures were done under fluorescent lighting of wavelengths above 500 nm. A2E was prepared according to published procedures and was used as a mixture of geometric isomers and was 98% pure as measured by high-performance liquid chromatography (HPLC).²⁵ Upon allowing the solid to stand at room temperature, in the dark, in a closed vial, for 4 months, two peaks appeared in reverse-phase chromatography that eluted before A2E. There was also a decreased absorbance as observed by UV–vis spectroscopy of the longer wavelength chromophore at 440 nm relative to the shorter wavelength chromophore with a maximum at 330 nm.

For liquid chromatography (LC) analysis, we used a Flexar FX-15 system with a PDA Detector (Perkin Elmer, Waltham, MA, USA), a 2.1 × 100 mm, 1.9 μm, C18 column (Brownlee, Perkin Elmer) and a 2.1 × 5-mm C18-guard column (Waters, Milford, MA, USA). The column oven was set to 45 °C and samples were eluted at 0.4 ml per minute with 60% by volume methanol containing 20% isopropanol and 0.01% trifluoroacetic acid (solvent A) and 40% type one water containing 0.01%

trifluoroacetic acid (solvent A) for 1 min. The gradient was changed to 95% solvent A over 4 min, further eluted for 3 min, increased to 100% solvent A over 1 min, and eluted for 4 min at 0.7 ml per minute. To generate a standard curve, we injected 1 μ l (272 pmoles), 2 μ l (544 pmoles), 4 μ l (1088 pmoles), and 6 μ l (1632 pmoles) of an A2E stock solution into a liquid chromatography (LC) system.

The seven human eyes (Baylor Lions Eye Bank, Houston, TX, USA) were from donors between 68 and 87 years of age. It was not known whether donors had any retinal disease. Eyes were stored wrapped in wet gauze, in air-tight containers, at 4 °C for 8 weeks before use. An initial incision was made on the cornea and the cornea–iris complex was cut off, 1–2 mm posterior to the corneal limbus. We removed the vitreous and lens, and collected the choroid, RPE, and neural retina of each eye into a 15-ml tube. The eyecup was washed with water to collect any pigmented tissue in the resulting eyecup. Samples were frozen at –78 °C and lyophilized at 30 °C for 12 h. The dehydrated tissues were placed in a 1.5-ml centrifuge tube. To the tube, we added 1 ml of ethanol, 0.6 g of 0.9–2.0 mm diameter steel beads, and the samples were homogenized (BBY24M Bullet Blender STORM, Next Advance, Averill Park, NY, USA setting 7, for 15 min). Samples were centrifuged for 5 min at 14 000 r.p.m., and the ethanol was removed and placed in a new tube. We added another 1 ml portion of ethanol, re-homogenized for 5 min and combined the sample with the first extract. Samples were vortexed for 30 s and solids were sedimented by centrifugation. We removed 1 ml of the ethanol extract and added it to a 1.5 ml capacity auto-sampler vial. Samples were held at 4 °C in an auto-sampler. We injected 30 μ l into the LC system. For quantification of A2E isomers, we compared LC peak areas at 445 nm with that of known concentrations of A2E isomers using the standard curve by integrating all-shown peaks and correlating the resulting total peak area with the amount of A2E injected into the column. Bovine eyes were treated similarly. Swine eyes were stored frozen at time to receipt, but otherwise treated similarly.

Preparation of liposomal retinaldehyde and A2E. All-*trans*-retinaldehyde (20 mg) and A2E (42 mg) were each dissolved in 1 ml of ethanol in two separate round-bottom flasks. A stock solution of L- α -Phosphatidylcholine (Sigma Aldrich number P5638, St. Louis, MO, USA) (365 mg), cholesterol (56 mg), and Tween 80 (252 mg) in 8 ml chloroform was made and 2 ml of this solution was put into the two flasks containing the actives and 2 ml into a new, 3rd flask as a control. The solvents were removed under vacuum with a rotary evaporator at 25 °C and trace solvents were removed by placing the flasks under high vacuum for 1 h then flushing each flask with argon. Flasks were charged with argon and 25 ml of saline was added to each. The solutions were stirred at 60 °C for 1 h to produce suspensions. Each solution was transferred to a 50-ml conical tube, placed on ice, and sonicated with a probe sonicator (15 s on/15 s off) for 5 min to yield transparent solutions. Tubes were filled to 50 ml with saline and centrifuged at 11 000 $\times g$ for 30 min, then filtered through a 0.2- μ m filter under sterile conditions. To determine the final concentrations, we added 10 μ l of the liposome to 1 ml of ethanol and recorded the absorption using ultraviolet–visible (UV–vis) spectroscopy (the absorbance equaled 0.52 for the aldehyde and 0.091 for A2E). We used extinction coefficients of 42 400 M⁻¹cm⁻¹ at 380 nm for the aldehyde⁶² and 15 140 M⁻¹cm⁻¹ at 433 nm for A2E. Retinaldehyde had an encapsulation efficiency of 86%, yielding final concentrations of 1.2 mM. A2E had a 58% encapsulation efficiency, yielding a final concentration of 0.83 mM. Solutions were stored at –20 °C.

We used HPLC to confirm that retinaldehyde and A2E did not oxidize, isomerize, or degraded during encapsulation. Both retinaldehyde and A2E gave the same chromatograms before and after their encapsulation. We did not observe degradation for either A2E or retinaldehyde when solutions were stored at –20 °C. For the retinaldehyde, a small amount of A2E formed by reaction with the phosphatidylethanolamine present in the lipids used for liposome formation. However, A2E formation accounted for less than 1% of total retinaldehyde and, thus, did not significantly change the concentration of retinaldehyde.

Retinal pigment epithelium cell models

Non-confluent cells: Cells (ARPE-19 from CRL-2302, American Type Culture Collection (ATCC), Manassas, VA, USA) were grown according to the manufacturer's instructions in Dulbecco's Modified Eagle medium/nutrient mixture F12 (DMEM/F12; BioWhittaker, Walkersville, MD, USA) with 10% fetal bovine serum (Fetal Bovine Serum, Standard Quality, PAA Laboratories, Etobicoke, Ontario, Canada) and 1% L-glutamine-penicillin-streptomycin (Sigma, St. Louis, MO, USA) at 37 °C and 5% CO₂. All assays were performed when the cells were approximately 80% confluent.

Two-week confluent cells: We grew the ARPE-19 cells in the above culture media supplemented with a bovine retinal extract at a final concentration of 500 μ g of protein/ml and cultured the cells up to 2 weeks after reaching confluence.

Eight-week confluent cells: ARPE-19 cells were plated onto gelatin-coated, 96-well plates. To prepare the gelatin-coated plates, we prepared a 1% gelatin solution by adding 2 g of gelatin to 200 ml of deionized water and autoclaved the solution for 45 min. The solution was placed under UV light while cooling to room temperature. We added 100 μ l of the gelatin solution to each well of a 96-well plate. The 96-well plates were placed into a 37 °C incubator for 30 min, after which non-adhered gelatin was removed and the plates were placed back in the incubator for another 30 min before plating the ARPE-19 cells. The cells were grown in culture media with bovine retinal extract at a final concentration of 500 μ g of protein/ml and cultured up to 8 weeks after reaching confluence. Four weeks after reaching confluence, the percent of fetal bovine serum was reduced to 1%.

Retinal extract: In total, 1–2 g of frozen bovine retina dark-adapted/dark-dissected (InVision BioResources, Lynnwood, WA, USA) was placed in 10 ml cold PBS with calcium and magnesium, and homogenized using a gentleMACS Dissociator (Miltenyi Biotec, Bergisch Gladbach, Germany) set to program-D. The homogenate was then centrifuged at 15 000 r.p.m. for 30 min at 4 °C and the supernatant was filtered through a 0.2- μ m cellulose nitrate, sterilization filter (Nalgene MF75, Rochester, NY, USA) and stored at –20 °C. Total protein was determined by measuring the absorbance at 280 nm, using bovine serum albumin as a standard.

Retinaldehyde metabolism in cultured RPE cells. We used 8-week confluent cells grown as described in a 6-well plate. However, the plate was not gelatin coated. We washed cells and added 600 μ l of cell media containing 100 μ M of liposomal retinaldehyde (64 pmoles of retinaldehyde/mm² of cells) to each well of the 6-well plate. Cells were incubated for up to 15 h. To stop the reaction and extract retinoids, we added 1 ml of butanol and scraped cells with the tip of a disposable pipette. We collected the solution, precipitated insoluble material by centrifugation at 15 000 r.p.m. for 5 min and analyzed the butanol layer by HPLC. HPLC was done on a Waters HPLC system with a 600 pump, a 2998 PDA detector with two silica, 3 μ m, 100 Å, 250 \times 2.0 mm columns (Phenomenex, Torrance, CA, USA) in series. Absorbance between 275 and 700 nm was recorded. We used a mobile phase of hexanes containing 0.5% isopropyl ether and 0.05% acetic acid at a flow rate of 1 ml per minute. Retinoids and retinoid isomers were identified by comparison of retention times⁶³ and absorbance spectra⁶³ to those of known retinoids. Relative retinoid concentrations were calculated by measuring the maximum absorbance of the eluted solvent, using the following extinction coefficients for hexanes: retinoic acid: 44 400,⁶⁴ retinol: 52 100,⁶⁵ 11-*cis*-retinol: 34 320,⁶⁵ and retinol esters: 52 100.⁶⁵

A2E uptake and stability in cultured RPE cells. We added 1000 μ l of a 15 μ M liposomal solution of A2E (16 pmoles of A2E/mm² of cells) to 2-week confluent cells grown as described in a 6-well plate. For controls, we added the same amount of A2E to wells with no cells. For analysis of A2E uptake, the media was removed and the cells were scraped from the surface with the tip of a 1 ml micropipette. We then added 1 ml ethanol to the well and collected the suspension in a 2-ml centrifuge tube. After centrifugation, we used HPLC to quantify A2E in the supernatant. For A2E stability, we treated cells for 4 days with 16 pmoles/mm² A2E, then replaced the media with media devoid of A2E. We then periodically quantified cellular A2E, as described above. All the experiments were run in triplicate for each data point.

Toxicity assessment of A2E and retinaldehyde. We grew ARPE-19 cells in 96-well plates as described. For the 8-week confluent assays, we added 29, 44, 59, 88, 117, 176, 234, 352, 469 and 703 pmoles of A2E or retinaldehyde per mm² of surface growth area. Each concentration was added to one column (eight wells/replicates). Column one was treated with media alone and column two with empty liposomes at a concentration corresponding to 703 pmoles A2E/mm².

Similarly, for the 2-week confluent assays, we treated cells with 23, 47, 94, 234 and 469 pmoles of A2E per mm² surface area. Each concentration was added to two columns (16 wells). Column one was treated with media alone and column two with empty liposomes at a concentration corresponding to 469 pmoles of A2E/mm².

For the non-confluent cells, we treated cells with 29, 44, 59, 88, 117, 176, 234 and 352 pmoles A2E/mm² surface area. Each concentration was added to one column (eight wells). Column one was treated with media alone and column two with empty liposomes as above. For the non confluent and 2-week confluent assays with retinaldehyde, we treated cells with 12, 23, 47, 164, 234, 352, 469, 703, 938 and 1172 pmoles retinaldehyde/mm² surface area. Column one was treated with media alone and column two with empty liposomes as above.

In all cases, we diluted the A2E, retinaldehyde, or empty liposomal stock solutions to the desired concentrations with culture media (DMEM/F12; with 10% fetal bovine serum). We removed the cell media and replaced it with media containing A2E or retinaldehyde at the above concentrations. We used the same volumes and otherwise identical experimental conditions for all treatments. Experiments were repeated in duplicate or triplicate (two or three plates) for each of the three cell culturing conditions and the two test compounds. Each concentration of A2E and retinaldehyde was tested in 16–24 replicates.

Morphological viability. ARPE-19 cells incubated with A2E and retinaldehyde were observed daily by phase-contrast microscopy at $\times 10$ magnification. Cells were scored dead when all cells in the viewing field, of all eight wells (one column), were rounded and swollen.

Resazurin assay. We measured cell viability using resazurin (7-hydroxy-3H-phenoazin-3-one-10-oxide), a non-fluorescent blue dye that is reduced by viable cells to the highly fluorescent resorufin. The rate of reduction is directly proportional to cell fitness.⁶⁶ Resazurin was prepared as a stock solution of 75 $\mu\text{g/ml}$ in calcium- and magnesium-free PBS and added to wells to give a final concentration of 10 $\mu\text{g/ml}$. Resorufin fluorescence was measured over 3 h using a microplate reader (SpectraMax Paradigm Multi-Mode Microplate Detection Platform, Molecular Devices LLC, Sunnyvale, CA, USA) by exciting at 530 nm and recording emission at 590 nm.

To obtain dose-response curves, we calculated resazurin reduction rates for each concentration of A2E or retinaldehyde by fitting the rate of resorufin appearance, from 40 min to 150 min, to regression lines (using GraphPad Prism, GraphPad Software, La Jolla, CA, USA). All regression fittings (over 1500 lines) gave $R^2 \geq 0.99$. For each plate, we normalized the reduction rates of the treated cells to control cells (empty liposomes or media alone).

Chronic exposure of A2E to cultured RPE cells. ARPE-19 cells were grown on microporous (8 μm) polycarbonate membrane inserts according to the manufacturer's instructions (Corning Costar, Catalog # 3422, Corning Incorporated Life Sciences, Tewksbury, MA, USA). Cells were seeded onto inserts at a density of 2.5×10^4 cells/well. After 5 days, inserts were transferred to a new 24-well plate, each well containing either 800 μl of a 2.5 μM solution of A2E in culture medium or culture medium with an equivalent amount of empty liposomes (controls). Media were changed to fresh media containing A2E or control liposomes every 10–12 days. After 3 weeks or 4 months, the cells were fixed and prepared for electron microscopy according to the manufacturer's instructions (Corning Costar, Catalog # 3422). Fluorescence microscopy images were acquired with an A1R MP Multiphoton And Confocal Microscope System (Nikon Instruments, Melville, NY, USA) using a $\times 40$ oil immersion objective. We processed images using ImageJ (National Institutes of Health, Bethesda, MD, USA).

For glycogen quantification, we fixed cells by immersion in cold (-20°C) methanol for 30 s. We used a commercial kit for glycogen staining (Periodic Acid-Schiff (PAS) Kit, Sigma, St. Louis, MO, USA) and quantified the resulting pararosaniline-Schiff base by confocal fluorescence microscopy. Periodic acid oxidized selectively 1,2-glycol linkages (HOCH₂-CH₂OH) of glycogen yielding aldehydes, which can be colored by condensation with pararosaniline.⁶⁷

Conflict of Interest

IW is a named inventor on a patent: Compositions and methods for treating macular degeneration (WO 2009035673 A8).

Acknowledgements. We thank the National Institute of Health, National Eye Institute (grant number 1R01EY021207-01) and the Brightfocus Foundation (grant number M2010096) for financial support.

1. Feeney-Burns L, Hilderbrand ES, Eldridge S. Aging human RPE: morphometric analysis of macular, equatorial, and peripheral cells. *Invest Ophthalmol Vis Sci* 1984; **25**: 195–200.
2. Eldred GE, Lasky MR. Retinal age pigments generated by self-assembling lysosomotropic detergents. *Nature* 1993; **361**: 724–726.
3. Murdaugh LS, Wang Z, Del Priore LV, Dillon J, Gaillard ER. Age-related accumulation of 3-nitrotyrosine and nitro-A2E in human Bruch's membrane. *Exp Eye Res* 2010; **90**: 564–571.
4. Weng J, Mata NL, Azarian SM, Tzekov RT, Birch DG, Travis GH. Insights into the function of Rim protein in photoreceptors and etiology of Stargardt's disease from the phenotype in abcr knockout mice. *Cell* 1999; **9**: 13–23.
5. Karan G, Lillo C, Yang Z, Cameron DJ, Locke KG, Zhao Y *et al*. Lipofuscin accumulation, abnormal electrophysiology, and photoreceptor degeneration in mutant ELOVL4 transgenic mice: a model for macular degeneration. *Proc Natl Acad Sci USA* 2005; **102**: 4164–4169.
6. Sparrow JR, Yoon KD, Wu Y, Yamamoto K. Interpretations of fundus autofluorescence from studies of the bisretinoids of the retina. *Invest Ophthalmol Vis Sci* 2010; **51**: 4351–4357.
7. Chan CC, Ross RJ, Shen D, Ding X, Majumdar Z, Bojanowski CM *et al*. Ccl2/Cx3cr1-deficient mice: an animal model for age-related macular degeneration. *Ophthalmic Res* 2008; **40**: 124–128.
8. Maeda A, Golczak M, Maeda T, Palczewski K. Limited roles of Rdh8, Rdh12, and Abca4 in all-trans-retinal clearance in mouse retina. *Invest Ophthalmol Vis Sci* 2009; **50**: 5435–5443.
9. De S, Sakmar TP. Interaction of A2E with model membranes. Implications to the pathogenesis of age-related macular degeneration. *J Gen Physiol* 2002; **120**: 147–157.
10. Iriyama A, Fujiki R, Inoue Y, Takahashi H, Tamaki Y, Takezawa S *et al*. A2E, a pigment of the lipofuscin of retinal pigment epithelial cells, is an endogenous ligand for retinoic acid receptor. *J Biol Chem* 2008; **283**: 11947–11953.
11. Zhou J, Jang YP, Kim SR, Sparrow JR. Complement activation by photooxidation products of A2E, a lipofuscin constituent of the retinal pigment epithelium. *Proc Natl Acad Sci USA* 2006; **103**: 16182–16187.
12. Finnemann S, Leung LW, Rodriguez-Boulan E. The lipofuscin component A2E selectively inhibits phagolysosomal degradation of photoreceptor phospholipid by the retinal pigment epithelium. *Proc Natl Acad Sci USA* 2002; **99**: 3842–3847.
13. Dontsov AE, Sakina NL, Bilinska B, Krzyzanowski L, Feldman TB, Ostrovsky MA. Comparison of photosensitizing effect of lipofuscin granules from retinal pigment epithelium of human donor eyes and their fluorophore A2E. *Dokl Biochem Biophys* 2005; **405**: 458–460.
14. Sparrow JR, Zhou J, Cai B. DNA is a target of the photodynamic effects elicited in A2E-laden RPE by blue-light illumination. *Invest Ophthalmol Vis Sci* 2003; **44**: 2245–2251.
15. Ben-Shabat S, Itagaki Y, Jockusch S, Sparrow JR, Turro NJ, Nakanishi K. Formation of a nonaioxirane from A2E, a lipofuscin fluorophore related to macular degeneration, and evidence of singlet oxygen involvement. *Angew Chem Int Ed Engl* 2002; **41**: 814–817.
16. Washington I, Jockusch S, Itagaki Y, Turro NJ, Nakanishi K. Superoxidation of bisretinoids. *Angew Chem Int Ed Engl* 2005; **44**: 7097–7100.
17. Yoon KD, Yamamoto K, Ueda K, Zhou J, Sparrow JR. A novel source of methylglyoxal and glyoxal in retina: implications for age-related macular degeneration. *PLoS ONE* 2012; **7**: e41309.
18. Moiseyev G, Nikolaeva O, Chen Y, Farjo K, Takahashi Y, Ma JX. Inhibition of the visual cycle by A2E through direct interaction with RPE65 and implications in Stargardt disease. *Proc Natl Acad Sci USA* 2010; **107**: 17551–17556.
19. Lukiw WJ, Mukherjee PK, Cui JG, Bazan NG. A2E selectively induces cox-2 in ARPE-19 and human neural cells. *Curr Eye Res* 2006; **31**: 259–263.
20. Thao MT, Renfus DJ, Dillon J, Gaillard ER. A2E-mediated photochemical modification to fibronectin and its implications to age-related changes in Bruch's membrane. *Photochem Photobiol* 2014; **90**: 329–334.
21. Fishkin N, Jang YP, Itagaki Y, Sparrow JR, Nakanishi K. A2-rhodopsin: a new fluorophore isolated from photoreceptor outer segments. *Org Biomol Chem* 2003; **1**: 1101–1105.
22. Bridges CD, Alvarez RA, Fong SL. Vitamin A in human eyes: amount, distribution, and composition. *Invest Ophthalmol Vis Sci* 1982; **22**: 706–714.
23. Uoshikami S, Noll GN. Isolated retinas synthesize visual pigments from tetinol congeners delivered by liposomes. *Science* 1978; **200**: 1393–1395.
24. Ma L, Kaufman Y, Zhang J, Washington I. C20-D3-vitamin A slows lipofuscin accumulation and electrophysiological retinal degeneration in a mouse model of Stargardt disease. *J Biol Chem* 2011; **286**: 7966–7974.
25. Parish CA, Hashimoto M, Nakanishi K, Dillon J, Sparrow J. Isolation and one-step preparation of A2E and iso-A2E, fluorophores from human retinal pigment epithelium. *Proc Natl Acad Sci USA* 1998; **95**: 14609–14613.
26. Bakall B, Radu RA, Stanton JB, Burke JM, McKay BS, Wadelius C *et al*. Enhanced accumulation of A2E in individuals homozygous or heterozygous for mutations in BEST1 (VMD2). *Exp Eye Res* 2007; **85**: 34–43.
27. Maeda A, Maeda T, Golczak M, Chou S, Desai A, Hoppel CL *et al*. Involvement of all-trans-retinal in acute light-induced retinopathy of mice. *J Biol Chem* 2009; **284**: 15173–15183.
28. Wielgus AR, Chignell CF, Ceger P, Roberts JE. Comparison of A2E cytotoxicity and phototoxicity with all-trans-retinal in human retinal pigment epithelial cells. *Photochem Photobiol* 2010; **86**: 781–791.

29. Suter M, Reme C, Grimm C, Wenzel A, Jaattela M, Esser P *et al*. Age-related macular degeneration. The lipofuscin component N-retinyl-N-retinylidene ethanolamine detaches proapoptotic proteins from mitochondria and induces apoptosis in mammalian retinal pigment epithelial cells. *J Biol Chem* 2000; **275**: 39625–39630.
30. Sparrow JR, Parish CA, Hashimoto M, Nakanishi K. A2E, a lipofuscin fluorophore, in human retinal pigmented epithelial cells in culture. *Invest Ophthalmol Vis Sci* 1999; **40**: 2988–2995.
31. Doyle JW, Dowgiert RK, Buzney SM. Factors modulating the effect of retinoids on cultured retinal pigment epithelial cell proliferation. *Curr Eye Res* 1992; **11**: 753–765.
32. Ablonczy Z, Dahrouj M, Tang PH, Liu Y, Sambamurti K, Marmorstein AD *et al*. Human retinal pigment epithelium cells as functional models for the RPE *in vivo*. *Invest Ophthalmol Vis Sci* 2011; **52**: 8614–8620.
33. Groenendijk GW, Jacobs CW, Bonting SL, Daemen FJ. Dark isomerization of retinals in the presence of phosphatidylethanolamine. *Eur J Biochem* 1980; **106**: 119–128.
34. Yang M, Fong HK. Synthesis of the all-trans-retinal chromophore of retinal G protein-coupled receptor opsin in cultured pigment epithelial cells. *J Biol Chem* 2002; **277**: 3318–3324.
35. Adler AJ, Edwards RB. Human interphotoreceptor matrix contains serum albumin and retinol-binding protein. *Exp Eye Res* 2000; **70**: 227–234.
36. Chen Y, Noy N. Retinoid specificity of interphotoreceptor retinoid-binding protein. *Biochemistry* 1994; **33**: 10658–10665.
37. Rak DJ, Hardy KM, Jaffe GJ, McKay BS. Ca²⁺ + -switch induction of RPE differentiation. *Exp Eye Res* 2006; **82**: 648–656.
38. Alge CS, Suppmann S, Priglinger SG, Neubauer AS, May CA, Hauck S *et al*. Comparative proteome analysis of native differentiated and cultured dedifferentiated human RPE cells. *Invest Ophthalmol Vis Sci* 2003; **44**: 3629–3641.
39. Kennedy BN, Goldflam S, Chang MA, Campochiaro P, Davis AA, Zack DJ *et al*. Transcriptional regulation of cellular retinaldehyde-binding protein in the retinal pigment epithelium. A role for the photoreceptor consensus element. *J Biol Chem* 1998; **273**: 5591–5598.
40. Lee SA, Belyaeva OV, Popov IK, Kedishvili NY. Overproduction of bioactive retinoic acid in cells expressing disease-associated mutants of retinol dehydrogenase 12. *J Biol Chem* 2007; **282**: 35621–35628.
41. Flood MT, Bridges CD, Alvarez RA, Blaner WS, Gouras P. Vitamin A utilization in human retinal pigment epithelial cells *in vitro*. *Invest Ophthalmol Vis Sci* 1983; **24**: 1227–1235.
42. Bridges CD, Alvarez RA, Fong SL, Gonzalez-Fernandez F, Lam DM, Liou GI. Visual cycle in the mammalian eye. Retinoid-binding proteins and the distribution of 11-cis retinoids. *Vision Res* 1984; **24**: 1581–1594.
43. Tendoess J, Alpern M, Lee GB, Heyner F. Some visual characteristics of Oguchi's disease. *Doc Ophthalmol* 1966; **20**: 406–419.
44. Rozanowska M, Handzel K, Boulton ME, Rozanowski B. Cytotoxicity of all-trans-retinal increases upon photodegradation. *Photochem Photobiol* 2012; **86**: 1362–1372.
45. Sparrow JR, Nakanishi K, Parish CA. The lipofuscin fluorophore A2E mediates blue light-induced damage to retinal pigmented epithelial cells. *Invest Ophthalmol Vis Sci* 2000; **41**: 1981–1989.
46. Boulton M, McKechnie NM, Breda J, Bayly M, Marshall J. The formation of autofluorescent granules in cultured human RPE. *Invest Ophthalmol Vis Sci* 1989; **30**: 82–89.
47. Wihlmark U, Wrigstad A, Roberg K, Brunk UT, Nilsson SE. Formation of lipofuscin in cultured retinal pigment epithelial cells exposed to pre-oxidized photoreceptor outer segments. *APMIS* 1996; **104**: 272–279.
48. Wihlmark U, Wrigstad A, Roberg K, Brunk UT, Nilsson SE. Lipofuscin formation in cultured retinal pigment epithelial cells exposed to photoreceptor outer segment material under different oxygen concentrations. *APMIS* 1996; **104**: 265–271.
49. Ben-Shabat S, Parish CA, Vollmer HR, Itagaki Y, Fishkin N, Nakanishi K *et al*. Biosynthetic studies of A2E, a major fluorophore of retinal pigment epithelial lipofuscin. *J Biol Chem* 2002; **277**: 7183–7190.
50. Feeney L. Lipofuscin and melanin of human retinal pigment epithelium. Fluorescence, enzyme cytochemical, and ultrastructural studies. *Invest Ophthalmol Vis Sci* 1978; **17**: 583–600.
51. Vives-Bauza C, Anand M, Shirazi AK, Magrane J, Gao J, Vollmer-Snarr HR *et al*. The age lipid A2E and mitochondrial dysfunction synergistically impair phagocytosis by retinal pigment epithelial cells. *J Biol Chem* 2008; **283**: 24770–24780.
52. Lullmann-Rauch R. Experimentally induced lipidosis in rat retinal pigment epithelium. A brief review. *Albrecht Von Graefes Arch Klin Exp Ophthalmol* 1981; **215**: 297–303.
53. Lerche W. [Electron-microscope studies of structural changes in the pigment epithelium of the human retina (author's transl)]. *Albrecht Von Graefes Arch Klin Exp Ophthalmol* 1974; **189**: 323–338.
54. Bairati A Jr, Orzalesi N. The ultrastructure of the pigment epithelium and of the photoreceptor-pigment epithelium junction in the human retina. *J Ultrastruct Res* 1963; **41**: 484–496.
55. Garron LK. The ultrastructure of the retinal pigment epithelium with observations on the choriocapillaris and Bruch's membrane. *Trans Am Ophthalmol Soc* 1963; **61**: 545–588.
56. John GB, Shang Y, Li L, Renken C, Mannella CA, Selker JM *et al*. The mitochondrial inner membrane protein mitofilin controls cristae morphology. *Mol Biol Cell* 2005; **16**: 1543–1554.
57. Feher J, Kovacs I, Artico M, Cavallotti C, Papale A, Balacco Gabrieli C. Mitochondrial alterations of retinal pigment epithelium in age-related macular degeneration. *Neurobiol Aging* 2006; **27**: 983–993.
58. McLeod DS, Taomoto M, Otsuji T, Green WR, Sunness JS, Luttly GA. Quantifying changes in RPE and choroidal vasculature in eyes with age-related macular degeneration. *Invest Ophthalmol Vis Sci* 2002; **43**: 1986–1993.
59. Green WR. Histopathology of age-related macular degeneration. *Mol Vis* 1999; **5**: 27.
60. Warburg O. Über die Klassifizierung tierischer Gewebe nach ihrem Stoffwechsel. *Biochem Ztschr* 1927; **184**: 484–488.
61. Senanayake P, Calabro A, Hu JG, Bonilha VL, Darr A, Bok D *et al*. Glucose utilization by the retinal pigment epithelium: evidence for rapid uptake and storage in glycogen, followed by glycogen utilization. *Exp Eye Res* 2006; **83**: 235–246.
62. Szuts EZ, Harosi FI. Solubility of retinoids in water. *Arch Biochem Biophys* 1991; **287**: 297–304.
63. Brinkmann E, Dehne L, Oei HB, Tiebach R, Baltes W. Separation of geometrical retinoid isomers in food samples by using narrow-bore high-performance liquid-chromatography. *J Chromatogr A* 1995; **693**: 271–279.
64. Newcomer ME, Ong DE. Purification and crystallization of a retinoic acid-binding protein from rat epididymis. Identity with the major androgen-dependent epididymal proteins. *J Biol Chem* 1990; **265**: 12876–12879.
65. Barua AB, Furr HC. Properties of retinoids. Structure, handling, and preparation. *Mol Biotechnol* 1998; **10**: 167–182.
66. McMillan MK, Li L, Parker JB, Patel L, Zhong Z, Gunnett JW *et al*. An improved resazurin-based cytotoxicity assay for hepatic cells. *Cell Biol Toxicol* 2002; **18**: 157–173.
67. Mc MJ. Histological and histochemical uses of periodic acid. *Stain Technol* 1948; **23**: 99–108.



Cell Death and Disease is an open-access journal published by Nature Publishing Group. This work is licensed under a Creative Commons Attribution-NonCommercial-ShareAlike 3.0 Unported License. The images or other third party material in this article are included in the article's Creative Commons license, unless indicated otherwise in the credit line; if the material is not included under the Creative Commons license, users will need to obtain permission from the license holder to reproduce the material. To view a copy of this license, visit <http://creativecommons.org/licenses/by-nc-sa/3.0/>

Supplementary Information accompanies this paper on Cell Death and Disease website (<http://www.nature.com/cddis>)